Published in final edited form as:
Cancer Res. 2014 January 1; 74(1): 341–352. doi:10.1158/0008-5472.CAN-13-1055.

Neuregulin autocrine signaling promotes self-renewal of breast tumor-initiating cells by triggering HER2/HER3 activation

Cleo Yi-Fang Lee[1], **Yuan Lin**[1], **Scott V. Bratman**[1], **Weiguo Feng**[1], **Angera H. Kuo**[1], **Ferenc A. Scheeren**[1], **Jesse M. Engreitz**[2], **Sushama Varma**[3], **Robert B. West**[3], and **Maximilian Diehn**[1,4,#]

[1]Stanford Cancer Institute and Institute for Stem Cell Biology and Regenerative Medicine, Stanford University School of Medicine, Stanford, California 94305, USA

[2]Harvard-MIT Division of Health Sciences and Technology, MIT, Cambridge, MA 02139, USA

[3]Department of Pathology, Stanford University School of Medicine, Stanford, California 94305, USA

[4]Department of Radiation Oncology, Stanford University School of Medicine, Stanford, California 94305, USA

Abstract

Currently only patients with HER2-positive tumors are candidates for HER2-targeted therapies. However, recent clinical observations suggest that the survival of patients with HER2-low breast cancers, who lack HER2 amplification, may benefit from adjuvant therapy that targets HER2. In this study, we explored a mechanism through which these benefits may be obtained. Prompted by the hypothesis that HER2/HER3 signaling in breast tumor-initiating cells (TICs) promotes self-renewal and survival, we obtained evidence that neuregulin 1 (NRG1) produced by TICs promotes their proliferation and self-renewal in HER2-low tumors, including in triple-negative breast tumors. Pharmacologic inhibition of EGFR, HER2 or both receptors reduced breast TIC survival and self-renewal in vitro and in vivo and increased TIC sensitivity to ionizing radiation. Through a tissue microarray analysis, we found that NRG1 expression and associated HER2 activation occurred in a subset of HER2-low breast cancers. Our results offer an explanation for why HER2 inhibition blocks the growth of HER2-low breast tumors. Moreover, they argue that dual inhibition of EGFR and HER2 may offer a useful therapeutic strategy to target TICs in these tumors. In generating a mechanistic rationale to apply HER2 targeting therapies in patients with HER2-low tumors, this work shows why these therapies could benefit a considerably larger number of breast cancer patients than they currently reach.

Keywords

breast cancer; tumor-initiating cells; HER2/HER3 signaling; neuregulin; lapatinib

INTRODUCTION

Breast cancer is the most common cancer and the leading cause of cancer deaths in women in North America (1). Breast cancers are heterogeneous and contain a subpopulation of cells called tumor-initiating cells (TICs; also called cancer stem cells - CSCs) that have the ability

[#]To whom correspondence should be addressed: diehn@stanford.edu, Phone: (650) 721-1550, Fax: (650) 723-8231.

No conflict of interest

to give rise to new tumors that recapitulate the full heterogeneity of the parental tumor. While aspects of the CSC hypothesis, such as which markers best identify CSCs and whether non-CSCs can acquire CSC properties, remain to be fully elucidated, a large number of studies have shown that breast CSCs can both self-renew and give rise to more differentiated non-tumorigenic cells (NTCs), which usually make up the bulk of a tumor (2–4). Markers including CD44, CD49f (ITGA6), and ALDH (ALDH1A1) can be used to highly enrich for tumorigenic activity (2, 3, 5–7). Furthermore, several studies have shown that TICs can preferentially survive conventional therapies such as radiotherapy and chemotherapy (8–10). Since eradication of all TICs within a tumor is essential in order to prevent tumor recurrence, therapeutic strategies targeting TICs will be critical to improving breast cancer patient survival.

Approximately 25% of all breast cancers are HER2 (ERBB2) positive by immunohistochemical analysis and its overexpression is associated with aggressive metastatic disease and historically poor clinical outcomes (11, 12). The HER family consists of four receptor members, EGFR, HER2, HER3 (ERBB3) and HER4 (ERBB4) and thirteen soluble HER family receptor ligands have been identified. Each has specific binding activities to one or more HER receptors (13). Upon ligand binding, the receptors are induced to form homodimers or heterodimers leading to transphosphorylation and activation of downstream signaling pathways. Neuregulins represent the largest subclass of HER receptor ligands and bind specifically to HER3 and HER4 (14).

Targeting HER2 in breast tumors that overexpress this gene as a result of gene amplification (i.e. HER2-positive cancers) represents one of the most important successes of molecularly targeted therapies in oncology and has resulted in dramatically improved outcomes for this subset of breast cancers (15). HER2 overexpression has also been linked to CSCs since exogenous overexpression of HER2 appears to increase numbers of CSCs and promotes mammary tumorigenesis and invasion and HER2 inhibition can target CSC-like cells (16–18). Intriguingly, while neoadjuvant treatment of HER2-low tumors with cytotoxic chemotherapy was found to preferentially spare breast CSCs, treatment of HER2-positive tumors with the HER2 inhibitor lapatinib resulted in a greater than 60% response rate and did not lead to accumulation of $CD44^{+}CD24^{-}$ cells, indicating that breast CSCs were killed (8). These results support the importance of HER2 in CSCs from HER2-positive tumors.

The role for HER2 targeting in the management of “HER2-low” breast cancers (i.e. HER2 expressed but non-amplified for *HER2* gene) remains controversial. While multiple trials have shown no benefit of targeting HER2 in metastatic HER2-low tumors, recent evidence suggests that HER2 inhibition may be beneficial in the adjuvant setting. Specifically, a retrospective analysis of the National Surgical Adjuvant Breast and Bowel Project (NSABP) trial B-31, which compared standard adjuvant chemotherapy with or without the anti-HER2 monoclonal antibody trastuzumab, found that HER2-low breast cancers benefited as much from HER2 targeting as HER2-positive breast cancers (19). Similarly, patients in the N9831 adjuvant trastuzumab trial whose tumors did not display *HER2* amplification by central review also seemed to benefit from trastuzumab (20). These intriguing results have led to the ongoing NSABP B-47 trial, which is testing the addition of trastuzumab to standard chemotherapy in HER2-low tumors.

The mechanism of how HER2 targeting could be of benefit in HER2-low tumors remains unclear. Therapies that increase cure rates in the adjuvant setting must be effective against TICs, since residual TICs would allow tumor re-growth. Based on this reasoning, we hypothesized that anti-HER2 therapies might target TICs in HER2-low breast cancer. We therefore set out to test the importance of HER2 signaling in breast TICs from primary HER2-low breast tumors.

MATERIALS AND METHODS

Reagents

Neutralizing antibodies used are: normal rabbit IgG (Santa Cruz, sc-2027), anti-mouse neuregulin 1 antibody (Santa Cruz, sc-28916), normal goat IgG (R&D, AB-108-C) and anti-human neuregulin 1 antibody (R&D, AF-296-NA). Accell SMARTpool mouse Her2 and Her3 siRNA was purchased from Thermo Scientific Dharmacon. Her2 specific inhibitors used are: AG825 (Tocris, #1555) and CP-724,714 (Selleck, S1167). Egfr specific inhibitor, erlotinib, was purchased from LC Laboratories (L-4007). Dual inhibitors of HER2 and EGFR used are: lapatinib (LC Laboratories, L-4804) and afatinib (Selleck, S1011). rhNRG1 was purchased from R&D Systems (#5898-NR-050).

Cell Labeling, Flow Cytometry and Cell Isolation

MMTV-*Wnt-1* murine mammary tumors were harvested and dissociated into single cell suspension as described previously (5, 10). Dissociated single cells were suspended at 1×10^7 per mL in staining buffer (HBSS with 2% heat-inactivated calf serum). Cells were first blocked with 10μg/μL rat IgG for 10 min., and then stained for 10 min. with the antibodies listed below. After washing, stained cells were re-suspended in staining buffer with 1μg/mL DAPI, analyzed, and sorted with a FACS Aria II cell sorter (BD Biosciences). The anti-mouse antibodies used in this study include CD45 (Ptprc)-Pacific Blue (1:200 dilution, Biolegend, #103126), CD31 (Pecam1)-Pacific Blue (1:200 dilution, Biolegend, #102422), CD24-PE (1:200 dilution, eBioscience, #12-0241-83), CD49f-PE-Cy5 (1:100 dilution, BD, #551129). Cells were sorted into staining buffer. The $CD24^{Hi}CD49f^{Hi}Lin^-$ and $CD24^{Lo}CD49f^{Lo}Lin^-$ subpopulations were defined as the top and bottom 10%, respectively.

Breast cancer cell line and drug treatments—Human breast cancer cell line SUM149 was kindly provided by Dr. Jonathan Pollack's laboratory (Stanford, CA) and cultured in HuMEC Ready Medium (Life Technology, #12752010). The cell line was authenticated by morphology, growth characteristics and FACS analysis. The day before drug treatment, cells were seeded in 6-well tissue culture plates. After cell attachment, different concentrations of erlotinib, AG825, or CP724,714 were added to the media and incubated in 37°C at 5% CO2. Four days after incubation, cells were collected and analyzed by flow cytometry for CD24, CD44, and EPCAM expression.

Quantitative RT-PCR Analysis

RNA was extracted from 5,000 sorted cells using RNeasy (Qiagen) and was reverse transcribed using the high-capacity RNA-to-cDNA kit (Applied Biosystems) according to manufacturer's instructions. Gene expression level was determined using Applied Biosystems 7900HT fast real-time quantitative PCR system using SYBR® Green PCR Master Mix (ABI). Each sample was normalized to the housekeeping gene Hprt and the relative expression level was determined. All primers used in this study were designed by IDT (www.idtdna.com) and synthesized by Elim Biopharm (www.elimbio.com). Primer sequences are listed in Supplemental Experimental Procedures.

Phospho-Flow Analysis

Breast TICs were starved in DMEM in 24-well low cluster plate for 30 min. and then stimulated with Nrg1 (100ng/mL) for 30min. at 37°C. Cells were then fixed with 4% paraformaldehyde (Electron Microscopy Sciences, #15710-S), washed with PBS buffer, permeabilized with ice cold methanol, washed twice with PBS buffer, and stained with the following antibodies and analyzed by FACS. Phospho-Akt (pT308)-PE (BD, #558275) and phospho-Erk1/2-(pT202/pY204)-PE-Cy7 (BD, #560116). For drug treatments, TICs were

pretreated with AG825 (100μM), CP-724,714 (5μM) and Lapatinib (5μM) for 10min at 37°C in DMEM and then stimulated with Nrg1 (100ng/mL). Cells were then fixed, permeabilized and analyzed by FACS.

Matrigel-Based 3-Dimensional Sphere Forming Assay

FACS-sorted MMTV-*Wnt1* tumor cells were re-suspended in culture medium consisting of DMEM/F12 (Invitrogen), 20 ng/mL mouse Egf (BD, #354001), 20 ng/mL human FGF (BD, #354060) plus 1x B27 (Invitrogen), and plated on top of a layer of solidified Matrigel (BD Biosciences). The culture medium was replenished every 3–4 days and spherical colonies (>50μm in diameter) were counted at 14 days. For the self-renewal assay, spherical colonies were dissociated with 1 mg/mL dispase (Invitrogen, #17105-041), digested with Trypsin/0.05% EDTA, and spheres were passaged through a 27-G needle five times to dissociate into single cells (21). Cells were then resuspended in culture medium, counted and re-plated on top of matrigel. For growing human xenograft spheroids, sorted cells were cultured in Advanced DMEM/F12 (Invitrogen) supplemented with 1x B27 (Invitrogen), 10 μM Y-27632 (Sigma), 20 ng/mL mouse Egf, 100 ng/mL human Noggin (Peprotech), 250 ng/mL human R-Spondin1 (R&D Systems), and plated on top of a layer of growth factor reduced matrigel (BD Bioscience) and a feeder layer of L-Wnt3a cells.

Tumor Growth Study and Limiting Dilution Analysis

FVB/NJ female mice (3–6 weeks of age) were anesthetized by inhalation of isoflurane (Baxter Healthcare Corporation, # NDC 10019-773-60) and tumor cells were mixed with 25% Matrigel (BD Bioscience) and injected percutaneously into mammary fat pads. When tumor size reached approximately 150 mm^3, mice were treated with DMSO or AG825 (50 μg/kg) via intraperitoneal injection (IP) daily and DMSO, erlotinib (100 mg/kb; once daily) or lapatinib (100 mg/kb; twice daily) via oral gavage (PO). Tumor size was measured by calipers twice a week. For LDA, treated tumors were then dissociated into single cells, analyzed by FACS and sorted $Lineage^-$ cells were injected back into syngeneic mice. After injection, mice were observed weekly for up to 3 months for tumor formation. Tumor-initiating cell frequencies and p-values were calculated using L-Calc (Vancouver, BC, Canada, http://www.stemcell.com). All animal experiments were conducted following the guidelines and protocols approved by Administrative Panel on Laboratory Animal Care (APLAC) at Stanford.

Human xenograft studies—Human xenograft tumor lines BCA70 and BCA71 were established by passaging tumor cells from a patient with triple negative breast cancer and passaged in NSG (NOD-scid $IL2Rg^{null}$) mice. The anti-human antibodies used were EPCAM-APC (1:50 dilution, BD, #347200) and CD49f-FITC (1:100 dilution, BD, #555735). Anti-mouse H2-Kd-PerCP-Cy5.5 (1:100 dilution, Biolegend, #116618) and CD45-PerCP-Cy5.5 (1:200 dilution, eBioscience, #45-9459-42) antibodies were used for depleting mouse cells.

Immunohistochemistry

Drug treated tumors were formalin-fixed, paraffin-embedded, and sectioned at 5μm thickness. Heat-induced antigen retrieval was performed by microwave oven for 25 minutes in citrate buffer. Sections were then blocked with normal serum (Vector Laboratories, PK-4001) for 1 hour at room temperature and incubated with primary antibodies at 4°C overnight. Primary antibodies used include 1:50 dilution of Neu (C-18) (Santa Cruz Biotechnology, Inc., sc-284), 1:50 dilution of p-Neu (Tyr 1248) (Santa Cruz Biotechnology, Inc., sc-293110), 1:50 dilution of EGF receptor (D38B1) (Cell Signaling Technology, #4267), and 1:1,600 dilution of phospho-EGFR (Tyr 1068) (Cell Signaling Technology,

#3777). Next day, sections were washed with Tris buffered saline (Fisher Scientific, BP24711) plus 0.001% Tween 20 (Sigma, P1379), incubated with 1:100 dilution of goat anti-rabbit IgG conjugated with DyLight 594 (Jackson Immunoresearch, #711-515-152) and visualized using a fluorescent microscope (Nikon Eclipse E800). The intensity of fluorescent staining was quantified by ImageJ (http://rsbweb.nih.gov/ij/). For tissue microarray IHC analysis, TA221 containing primary breast carcinoma samples used was previously described (22). Primary antibodies used were: 1:100 dilution of HER2 (CB11) (Biogenex), 1:50 dilution of NRG1 (7D5) (Thermo Scientific) and 1:25 dilution of pHER2 (Cell Signaling Technology, #2243). For unbiased and reproducible quantification of IHC staining patterns, we utilized GemIdent, a supervised *in silico* image segmentation system (23). GemIdent was applied to digital images of TMA specimens to generate separate image masks of both IHC localization ("stain") and non-tissue empty space ("background"). For each IHC stain, paired stain and background image masks were processed to calculate the staining fraction of each TMA specimen.

Statistical Analysis

Statistical analysis was performed using the unpaired student t test and p values less than 0.05 were considered statistically significant.

RESULTS

Analysis of Her2/Her3 signaling in Her2-low mammary TICs

To explore the role of Her2 signaling in TICs within Her2-low tumors we began by studying mammary tumors arising in MMTV-*Wnt1* transgenic mice. These tumors have previously been shown to contain a subpopulation of TICs that can be identified using various combinations of surface markers including CD24, CD49f, Thy1, and CD61 (Itgb3) (5, 24). Since functional verification of TIC activity in purported TIC-enriched populations is critical, we began by confirming that $CD24^{Hi}CD49f^{Hi}Lin^{-}$ cells within these tumors are highly enriched for TICs (25). *In vivo* limiting dilution analyses revealed that $CD24^{Hi}CD49f^{Hi}Lin^{-}$ cells were approximately 10- and 100-fold enriched for tumor-initiating activity compared to the Lin^{-} and $CD24^{Lo}CD49f^{Lo}Lin^{-}$ subpopulations, respectively ($p < 0.001$; Fig. S1A and S1C). The TIC frequency in the middle subpopulation ($CD24^{Med}CD49f^{Med}Lin^{-}$) was intermediate between the other two subpopulations, indicating partial overlap of TIC and NTC subpopulations in this region (Fig. S1C). Real-time PCR analysis showed the TIC-enriched subpopulation predominantly expressed basal cell markers (Trp63 and Krt5) whereas the NTC subpopulation exhibited higher expression of the luminal cell marker, Krt18 (Fig. S1B). Tumors arising from $CD24^{Hi}CD49f^{Hi}Lin^{-}$ cells contained the full phenotypic heterogeneity of the parental tumors and could be passaged for multiple generations (Fig. S1D). Furthermore, we established that $CD24^{Hi}CD49f^{Hi}Lin^{-}$ TIC-enriched cells isolated from MMTV-*Wnt-1* tumors were clonogenic in an *in vitro* 3D matrigel-based tumor sphere assay, whereas $CD24^{Lo}CD49f^{Lo}Lin^{-}$ NTCs formed no or very few tumor spheroids. The frequency of sphere forming cells *in vitro* and tumor initiating cells *in vivo* within the $CD24^{Hi}CD49f^{Hi}Lin^{-}$ subpopulation was similar at approximately 1 in 70, suggesting that this culture system could serve as an *in vitro* surrogate for tumor initiation (Fig. S1E).

Clinically, breast cancers are classified as HER2+ if increased copy numbers of the *HER2* locus are detected by fluorescent *in situ* hybridization (26). To similarly assess the Her2 status of MMTV-*Wnt1* tumors, we performed qPCR for the *Her2* locus in tumor and normal cells and found that, as expected, it was not amplified in these tumors (Fig. 1A). However, as in many HER2-neagive human breast cancers (19), Her2 mRNA was detectable by quantitative real time polymerase chain reaction (qRT-PCR, Fig. 1B) and Her2 protein was

detectable by immunofluorescence analysis (see below). More detailed examination of the expression levels of Her family receptors revealed that both TICs and NTCs expressed Egfr, Her2 and Her3, with expression generally being greater in NTCs (Fig. 1B). Expression of Her2 and Her3 was approximately 5- to 8-fold higher in TICs than $CD24^{Hi}CD49f^{Hi}Lin^{-}$ cells from normal mammary glands, which are enriched for mammary stem cells or so called mammary repopulation units (MRUs, $p<0.03$; Fig. 1B) (27, 28). We also examined expression of Her2-family ligands. Nrg1 and Nrg2 mRNA levels were greater than 2- and 6-fold higher in TICs as compared to MRU-enriched cells and NTCs, respectively ($p<0.04$; Fig. 1C).

The overexpression of Nrg1 and Nrg2 in TICs suggested that TICs may activate Her2/Her3 signaling in an autocrine fashion. Since neuregulins activate Her2/Her3 heterodimers and lead to the phosphorylation and activation of Akt (Akt1) and Erk1/2 (Mapk3/1), we next examined phosphorylation of Akt and Erk1/2 in TICs by phospho-flow analysis. Phosphorylation was observed in both $CD24^{Hi}CD49f^{Hi}Lin^{-}$ TIC-enriched cells and NTCs, consistent with both populations expressing Her2 and Her3. However, Her2 phosphorylation was 30% higher and phosphorylated Akt and Erk1/2 levels were more than 2-fold higher in the TIC-enriched subpopulation compared to NTCs ($p<0.001$; Fig. 1D, 1E). This suggested that autocrine activation of Her2/Her3 signaling may govern biological activity of breast TICs.

Nrg1 enhances tumor sphere-forming capacity of mammary TICs

To determine whether Nrg1 can stimulate the tumor sphere-forming capacity of mammary TICs, $CD24^{Hi}CD49f^{Hi}Lin^{-}$ TIC-enriched cells were purified by flow cytometry and treated with recombinant Nrg1 or a neutralizing antibody targeting endogenous Nrg1 in the 3-dimensional tumor spheroid forming assay. A greater than two-fold increase in the number of spheres was observed in $CD24^{Hi}CD49f^{Hi}Lin^{-}$ TIC-enriched cells treated with Nrg1 ($p<0.05$; Fig. 2A). Nrg1 treatment had no discernible effect on $CD24^{Lo}CD49f^{Lo}Lin^{-}$ NTCs, as no spheroids formed in its presence or absence (data not shown). Significantly, treatment of TIC cultures with anti-Nrg1 antibody in the absence of exogenous Nrg1 resulted in a 70% reduction in sphere formation ($p<0.001$; Fig. 2B). Furthermore, siRNA-mediated knockdown of Her2 and Her3 decreased the number of spheroids by 70% and 25% compared to control siRNA respectively, consistent with a similar reduction in mRNA levels ($p<0.04$; Fig. 2C). Phospho-flow analysis of downstream effector kinases in TICs further revealed a 50% increase in the phosphorylation level of Akt and Erk1/2 by Nrg1 stimulation ($p<0.05$; Fig. 2D) and Nrg1-mediated activation of Akt and Erk1/2 was inhibited when $CD24^{Hi}CD49f^{Hi}Lin^{-}$ TIC-enriched cells were pre-treated with specific inhibitors of Her2, including AG825, CP-724,714, and the dual Egfr/Her2 inhibitor lapatinib ($p<0.05$; Fig. 2E). These results indicate that Nrg1 promotes proliferation and survival of $CD24^{Hi}CD49f^{Hi}Lin^{-}$ TIC-enriched cells through activation of Her2/Her3 and subsequent stimulation of downstream Akt and MAPK pathways.

Inhibition of Her2 and Egfr targets mammary TIC clonogenicity and self-renewal

Active Her2/Her3 signaling in $CD24^{Hi}CD49f^{Hi}Lin^{-}$ TIC-enriched cells suggested that Her2 inhibition may target TICs in HER2-low breast cancers. Additionally, an *in silico* search for differential expression patterns that mimic the global gene expression changes between TICs and NTCs using ProfileChaser (29) identified AG825, a Her2-inhibitor, as the most highly significant pharmacologic agent, with AG825-treated cells more closely resembling NTCs while vehicle treated cells more closely resembled TICs (data not shown). We therefore investigated the effects of two specific inhibitors of Her2, AG825 and CP-724,714, on TIC sphere formation (30, 31). $CD24^{Hi}CD49f^{Hi}Lin^{-}$ TIC-enriched cells treated with either inhibitor formed smaller and fewer spheres than control cells (Fig. 3A, 3C) and a greater

than 70% reduction in the number of spheres was observed at 25μM of AG825 and 10μM of CP-724,714 ($p<0.03$; Fig. 3B, 3D). Since Egf is a component of the tumor sphere media, we hypothesized that Egfr inhibition would also target TICs. Thus, we tested the effect of Egfr inhibition on tumor sphere formation, and found that erlotinib at 10μM killed more than 70% of TICs ($p<0.002$; Fig. 3E, 3F). Thus, inhibition of Her2 and Egfr suppresses sphere-forming ability of breast TICs *in vitro*.

Given the effects of inhibiting Her2 and Egfr that we observed, we next evaluated simultaneous targeting of the two receptors using the clinically available dual Her2 and Egfr inhibitors afatinib and lapatinib on TIC clonogenicity and self-renewal. As with the other inhibitors, we found that afatinib and lapatinib inhibited the sphere-forming ability of $CD24^{Hi}CD49f^{Hi}Lin^{-}$ TIC-enriched cells in a concentration dependent manner with a greater than 80% reduction in the number of surviving spheres at a concentration of 1 μM and 2.5 μM, respectively ($p<0.03$; Fig. 4A, 4B). The sensitivity of TICs is similar to recently described cancer cell lines that lack HER2 amplification but are responsive to lapatinib (32). FACS analysis of dissociated spheres revealed a reduction of the TIC subpopulation from an average of 16% to 3% in tumor cells treated with lapatinib ($p<0.002$; Fig. 4C). To test whether Her2 and Egfr inhibition reduced TIC self-renewal, we tested the effect of lapatinib in an *in vitro* self-renewal assay. In this assay, $CD24^{Hi}CD49f^{Hi}Lin^{-}$ TIC-enriched cells purified from tumors were exposed to lapatinib during the first passage and then dissociated and re-plated in fresh media lacking lapatinib in the second passage. We found that lapatinib had a strong effect on $CD24^{Hi}CD49f^{Hi}Lin^{-}$ TIC-enriched cell self-renewal and reduced spheroid-forming frequency in the second passage by 5-fold at a concentration of 1 μM ($p<0.04$; Fig. 4D). These results indicate that dual inhibition of Her2 and Egfr can target TIC self-renewal in HER2-low tumors.

Inhibition of Her2 and Egfr targets mammary TICs *in vivo*

To evaluate the effect of Her2 inhibition on TICs *in vivo*, mice bearing MMTV-*Wnt-1* tumors were treated with DMSO or AG825 via daily intraperitoneal injections for 14 days. AG825 treatment caused minimal growth delay (Fig. 5A). At the end of treatment, the frequency of $CD24^{Hi}CD49f^{Hi}$ TIC enriched cells was reduced by 2-fold as assessed by FACS ($p<0.002$; Fig. 5B). Since TIC-enriched subpopulations are not entirely pure and since *in vitro* assays may not accurately reflect tumor-initiating activities, we next wished to confirm effects of Her2 inhibition on TIC self-renewal *in vivo*. If HER2 pathway regulates TICs self-renewal, then HER2 inhibition should decrease *in vivo* tumor initiating activity. Therefore, we performed limiting dilution analyses (LDA) of control and treated tumors. Tumors from animals treated with vehicle or drug were dissociated and lineage negative tumor cells were used for secondary transplants to functionally test if AG825 treatment led to a reduction of TICs. LDA revealed a greater than 4-fold reduction in breast TIC frequency (measured by tumor initiating activity) in the AG825 treatment group as compared to the control group, consistent with the percent change in TICs observed by flow cytometry ($p<0.01$; Table 1, Fig. 5B). This confirmed that Her2 inhibition by AG825 inhibits TIC self-renewal *in vivo*.

To test whether a similar effect could be observed with Egfr inhibition or dual Her2/Egfr inhibition, tumor bearing animals were treated with DMSO, erlotinib (once daily), or lapatinib (twice daily) via oral gavage for 14 days. Erlotinib treatment led to roughly similar tumor growth delay as AG825 and by day 14 the treated tumors were 1.7-fold smaller than the control group ($p<0.01$; Fig. 5A). By comparison, lapatinib treatment led to more significant growth delay and by day 14 lapatinib treated tumors were 3.5-fold smaller than vehicle-treated tumors ($p<0.001$; Fig. 5A). FACS analysis of tumors treated with erlotinib and lapatinib showed a 50% reduction of the $CD24^{Hi}CD49f^{Hi}$ TIC-enriched subpopulation

compared to the control group ($p<0.02$; Fig. 5B). As before, we also performed LDA to confirm that erlotinib and lapatinib inhibits self-renewal of TICs *in vivo*. Secondary *in vivo* transplantation of cells from treated tumors revealed an approximately four- and six-fold reduction in mammary TIC frequency in the erlotinib and lapatinib treated group as compared to the control group, respectively, confirming *in vivo* activity against TICs (Table 1). Immunohistochemical analysis confirmed that both AG825 and lapatinib reduced the level of phosphorylated Her2 by 40%, while only erlotinib and lapatinib treatment caused reduction of phosphorylated Egfr ($p<0.05$; Fig. 5C, 5D). Thus, inhibition of Her2, Egfr, or both targets TICs in Her2-low MMTV-*Wnt-1* mammary tumors *in vivo*.

HER2 and EGFR inhibition targets TICs in human HER2-low breast cancer

We next sought to determine whether observations made using murine mammary tumors could be replicated with human HER2-low breast cancers. Lapatinib treatment of a large panel of cancer cell lines was recently reported as part of the Cancer Cell Line Encyclopedia (33). This data set included cell lines with and without *HER2* amplification and as expected, all *HER2* amplified cell lines were sensitive to lapatinib. However, some cell lines lacking *HER2* amplification were also sensitive to lapatinib. Strikingly, the sensitive non-*HER2* amplified cell lines all displayed overexpression of HER3 (Fig. 6A). NRG1, NRG2, and HER2 were also expressed in all of the sensitive *HER2*-non-amplified cell lines, suggesting autocrine activation of HER2/HER3 (Fig. S2). Interestingly, all sensitive non-*HER2* amplified cell lines (HDQP1, Cal851, HCC1806, MDA-MB-468, MDA-MB-175-VII) originated from triple negative tumors. These data indicate that a subset of human breast cancer cell lines is sensitive to lapatinib in the absence of *HER2* amplification and suggest that this effect may be mediated via HER3 signaling.

To more specifically test the effect of HER2 inhibition on human breast cancer TIC-like cells, we next tested HER2 inhibition using the triple negative *HER2*-non-amplified inflammatory breast cancer cell line SUM149, which contains both $EPCAM^+$ luminal-like cells and $EPCAM^-$ cells. While it is controversial if established breast cancer cell lines contain true surrogates of primary TICs, a previous study suggested that EPCAM- cells within SUM149 bulk populations have TIC-like characteristics (34). Pharmacological inhibition of HER2 by AG825 or CP-724,714 reduced the percentage of the $EPCAM^-$ TIC-like subpopulation in SUM149 cell line by greater than 3 and 2-fold, respectively (Fig. S3).

Next, we wished to confirm an effect of HER2 inhibition on TICs in early passage, HER2-low breast cancer patient-derived xenografts, which represent the best accepted preclinical model of human breast cancer TICs. Given the observation noted above that a subset of triple negative breast cancer cell lines was sensitive to lapatinib, we examined two independent triple negative human breast cancer patient-derived xenografts lines (BCA70 & BCA71) that were established directly from a surgical specimen and never passaged *in vitro*. LDA analysis using BCA70 revealed that TICs were over 180-fold enriched in the $EPCAM^+CD49f^+$ subpopulation compared to the $EPCAM^-CD49f^-$ subpopulation ($p = 0.0001$; Fig. S4A, S4B). Analogously to MMTV-*Wnt-1* mammary tumors, $EPCAM^+CD49f^+$ TIC-enriched cells gave rise to tumor spheres in 3-dimensional culture while non-tumorigenic cells did not (Fig. S4C). EGFR, HER2, and HER3 were expressed in a similar pattern as in MMTV-*Wnt-1* tumors and NRG1 was expressed by both subpopulations (Fig. 6B). NRG1 treatment of $EPCAM^+CD49f^+$ TIC-enriched cells from both BCA70 and BCA71 xenografts resulted in a 2-fold increase in the number of spheres ($p<0.01$; Fig. 6C), whereas treatment with anti-NRG1 antibody reduced sphere formation by greater than 30% ($p<0.01$; Fig. 6D). This suggested that as with mammary TICs, human breast TICs rely on NRG1 to promote their self-renewal.

To test the effect of inhibiting Her2 and Egfr on human TICs in triple negative breast cancers we next exposed these cells to the same inhibitors used above for murine TICs. Treatment of $EPCAM^{+}CD49f^{+}$ TIC-enriched cells with AG825, CP-724,714, erlotinib, lapatinib or afatinib strongly inhibited tumor spheroid formation in both xenograft lines ($p<0.02$; Fig. 6E, 6F, S5A–S5D), suggesting that breast TICs are sensitive to inhibition of both HER2 and EGFR. Since HER2 and EGFR inhibition at clinically relevant doses did not eliminate all TICs, we also tested whether the combination of dual HER2 and EGFR inhibition and radiotherapy could further increase killing of TICs. $EPCAM^{+}CD49f^{+}$ TIC-enriched cells treated with lapatinib or afatinib in combination with a clinically relevant dose of ionizing radiation (2 Gy) were more sensitive to radiation (Fig. 6F, S5D). This suggests that combination therapy could be an effective strategy for targeting TICs in the clinic.

Finally, in order to determine if we could find evidence of NRG1/HER2 pathway activation in other HER2-low breast cancers, we analyzed expression of NRG1, pHER2 and HER2 in HER2-low breast cancers by immunohistochemical staining of a tissue microarray containing 132 Stage I-III HER2-low (FISH-negative and IHC score <2) breast cancers. Twenty-one (19%) tumors displayed NRG1 expression at greater than 5%, and these tumors were significantly enriched for expression of pHER2 ($p<0.04$; Fig. 6G–H). Using a 10% cutoff of NRG1 expression revealed an even stronger correlation between NRG1 and pHER2 expression ($p<0.005$; Fig. 6H).

DISCUSSION

The existence of TICs has important implications for rational design of therapies, since these cells must be eliminated or inactivated in order to achieve cure. While novel therapeutic agents are clearly needed, clinical experience using existing agents can help identify currently available treatments that target TICs. Specifically, therapies that increase cure rates in the adjuvant setting must by definition be effective against TICs. Therefore, given the clinical observations of therapeutic benefit of trastuzumab in this group of breast cancers (19, 20), we hypothesized that anti-HER2 therapies might target TICs in HER2-low tumors. In this study, we show that neuregulins activate the HER2/HER3 pathway in breast TICs to promote self-renewal in HER2-low breast cancers and that dual inhibition of EGFR and HER2 is more effective than targeting either alone. Furthermore, this mechanism also holds true for triple negative breast cancer cell lines and two triple negative patient-derived xenografts. While it is not clear if HER2 is absolutely required for tumor initiation in the primary tumor models we studied, inhibiting receptor either extracellularly or intracellularly using clinically-available drugs inhibits TIC self-renewal, both *in vitro* and *in vivo*. Thus, this NRG1-mediated HER2 activation serves as a potential explanation for the clinical efficacy of HER2 targeting in HER2-low tumors.

Several previous studies have suggested a potential role for HER2 in HER2-low tumors. For instance, NRG1 has been shown to promote tumor formation and metastasis of HER2-low human breast cancer cell lines, including triple negative cell lines (35, 36). Furthermore, it was recently shown that exogenous NRG1 promotes mammosphere formation in established cell lines and cultured cells from primary breast cancer tissues (37). Finally, side population and ALDEFLUOR-positive cells from luminal (ER+/PR+, HER2-) breast cancer cell lines have been shown to be sensitive to HER2 inhibition (38, 39).

Our work differs from the previous studies in several important ways. First, we describe a novel mechanism involving neuregulin-mediated activation of HER2 in TICs from these tumors. While normal mammary stem cells express low levels of neuregulins, breast TICs express significantly higher levels, suggesting that autocrine and/or paracrine signaling by neuregulins promotes the uncontrolled growth of TICs that is a hallmark of cancer. Second,

we focused on TICs purified directly from murine mammary tumors or patient-derived xenografts since it remains unclear how well TIC-like cells in established cell lines reflect properties of TICs found in primary tumors such as those used in our study (25, 40). Third, we show that HER2-signaling is functionally important in TICs from triple negative breast cancers, for which effective targeted therapies remain elusive. Finally, we found that dual inhibition of HER2 and EGFR appears to be more effective than inhibition of either receptor alone and leads to TIC radiosensitization, which has important implications for the design of clinical trials.

Clinical data regarding the efficacy of anti-HER2 therapies in HER2-low breast cancers are mixed. Retrospective analyses of trials using trastuzumab in the adjuvant setting have suggested that patients with HER2-low tumors may benefit from this class of agents (19, 20). Conversely, HER2-targeted therapies in patients with metastatic HER2-low tumors have generally not been effective. However, retrospective analysis of neuregulin expression in patients with metastatic HER2-low breast cancers treated with trastuzumab plus taxanes showed improved time to disease progression in patients whose tumors expressed high levels of NRG, suggesting that NRG expression may predict response to trastuzumab-based therapies (41). Using TMA analysis we found that a significant subset of Stage I-III HER2-low tumors express NRG1 and these tumors tend to display phosphorylated HER2. This suggests that stratification of HER2-low patients by expression of neuregulin and/or phosphorylated HER receptors may allow identification of a subset of patients who could benefit from HER2-targeted therapies (41–43).

Our results suggest several possible explanations for the disparate clinical results in the adjuvant and metastatic settings. First, TICs in microscopic tumor deposits present in the adjuvant setting may be more dependent on HER2 signaling than TICs in macroscopic tumors present in patients with metastatic disease. For example, clinically-detectable metastatic tumors may have acquired additional mutations that reduce the reliance of their TICs on the HER2 pathway, thus leading to the observed lack of benefit of HER2 targeting in most patients with metastatic HER2-low breast cancer. Secondly, TICs in only a subset of HER2-low tumors may rely on neuregulin-mediated activation of the HER pathway, thus causing previous trials to be underpowered to observe an effect. This notion is supported by our observation that lapatinib has significant activity in only a subset of HER2-low breast cancer cell lines included in the Cancer Cell Line Encyclopedia and that only a subset of HER2-low tumors expressed NRG in our TMA analysis. Finally, it is possible that HER2 targeted agents reach insufficient tissue levels in grossly visible HER2-low tumors and thus are less effective than in microscopic deposits present in the adjuvant setting.

While TIC frequency significantly decreased after HER2 inhibition, it was not reduced to zero. This suggests that HER2-targeted therapy of HER2-low tumors would be most effective when combined with other therapies such as radiotherapy or chemotherapy. Indeed, we found that lapatinib and afatinib increased sensitivity of TICs to radiation, providing a rationale for combining HER pathway inhibition with radiation therapy to target these cells.

In conclusion, we demonstrated that TICs in at least a subset of HER2-low breast cancers are driven to self-renew by expression of neuregulin and activation of the HER pathway and that inhibition of HER2, EGFR, or both target breast TICs. Our findings offer a potential explanation for the benefit of HER2-targeted therapies in patients with HER2-low breast cancers. Activation of oncogenic signaling pathways in the absence of somatic genetic alterations in these pathways may be a common mechanism by which TICs promote self-renewal and present a potential opportunity for developing individualized, TIC-targeted therapeutic strategies.

Supplementary Material

Refer to Web version on PubMed Central for supplementary material.

Acknowledgments

We thank Patty Lovelace for maintaining the FACS facility and Jessica Lam for technical assistance. This work was supported by grants from the National Institutes of Health (M.D. - P30CA147933; P01CA139490), the Mallinckrodt Foundation (M.D.), Nadia's Gift (M.D.), the Virginia and D.K. Ludwig Foundation (M.D.), and the CRK Faculty Scholar Fund. M.D. is supported by a Doris Duke Clinical Scientist Development Award. C.Y.-F. Lee is supported by a Canadian Institutes of Health Research postdoctoral fellowship award (Eileen Iwanicki Fellowship in Breast Cancer Research).

References

1. Siegel R, Naishadham D, Jemal A. Cancer statistics, 2012. CA Cancer J Clin. 2012; 62:10–29. [PubMed: 22237781]
2. Al-Hajj M, Wicha MS, Benito-Hernandez A, Morrison SJ, Clarke MF. Prospective identification of tumorigenic breast cancer cells. Proc Natl Acad Sci U S A. 2003; 100:3983–8. [PubMed: 12629218]
3. Ginestier C, Hur MH, Charafe-Jauffret E, Monville F, Dutcher J, Brown M, et al. ALDH1 is a marker of normal and malignant human mammary stem cells and a predictor of poor clinical outcome. Cell Stem Cell. 2007; 1:555–67. [PubMed: 18371393]
4. Ponti D, Costa A, Zaffaroni N, Pratesi G, Petrangolini G, Coradini D, et al. Isolation and in vitro propagation of tumorigenic breast cancer cells with stem/progenitor cell properties. Cancer Res. 2005; 65:5506–11. [PubMed: 15994920]
5. Cho RW, Wang X, Diehn M, Shedden K, Chen GY, Sherlock G, et al. Isolation and molecular characterization of cancer stem cells in MMTV-Wnt-1 murine breast tumors. Stem Cells. 2008; 26:364–71. [PubMed: 17975224]
6. Lo PK, Kanojia D, Liu X, Singh UP, Berger FG, Wang Q, et al. CD49f and CD61 identify Her2/neu-induced mammary tumor-initiating cells that are potentially derived from luminal progenitors and maintained by the integrin-TGFbeta signaling. Oncogene. 2012; 31:2614–26. [PubMed: 21996747]
7. Zhang M, Behbod F, Atkinson RL, Landis MD, Kittrell F, Edwards D, et al. Identification of tumor-initiating cells in a p53-null mouse model of breast cancer. Cancer Res. 2008; 68:4674–82. [PubMed: 18559513]
8. Li X, Lewis MT, Huang J, Gutierrez C, Osborne CK, Wu MF, et al. Intrinsic resistance of tumorigenic breast cancer cells to chemotherapy. J Natl Cancer Inst. 2008; 100:672–9. [PubMed: 18445819]
9. Phillips TM, McBride WH, Pajonk F. The response of CD24(-/low)/CD44+ breast cancer-initiating cells to radiation. J Natl Cancer Inst. 2006; 98:1777–85. [PubMed: 17179479]
10. Diehn M, Cho RW, Lobo NA, Kalisky T, Dorie MJ, Kulp AN, et al. Association of reactive oxygen species levels and radioresistance in cancer stem cells. Nature. 2009; 458:780–3. [PubMed: 19194462]
11. Al-Kuraya K, Schraml P, Torhorst J, Tapia C, Zaharieva B, Novotny H, et al. Prognostic relevance of gene amplifications and coamplifications in breast cancer. Cancer Res. 2004; 64:8534–40. [PubMed: 15574759]
12. Slamon DJ, Clark GM, Wong SG, Levin WJ, Ullrich A, McGuire WL. Human breast cancer: correlation of relapse and survival with amplification of the HER-2/neu oncogene. Science. 1987; 235:177–82. [PubMed: 3798106]
13. Baselga J, Swain SM. Novel anticancer targets: revisiting ERBB2 and discovering ERBB3. Nat Rev Cancer. 2009; 9:463–75. [PubMed: 19536107]
14. Falls DL. Neuregulins: functions, forms, and signaling strategies. Exp Cell Res. 2003; 284:14–30. [PubMed: 12648463]

15. Arteaga CL, Sliwkowski MX, Osborne CK, Perez EA, Puglisi F, Gianni L. Treatment of HER2-positive breast cancer: current status and future perspectives. Nat Rev Clin Oncol. 2012; 9:16–32. [PubMed: 22124364]
16. Magnifico A, Albano L, Campaner S, Delia D, Castiglioni F, Gasparini P, et al. Tumor-initiating cells of HER2-positive carcinoma cell lines express the highest oncoprotein levels and are sensitive to trastuzumab. Clin Cancer Res. 2009; 15:2010–21. [PubMed: 19276287]
17. Chakrabarty A, Bhola NE, Sutton C, Ghosh R, Kuba MG, Dave B, et al. Trastuzumab-resistant cells rely on a HER2-PI3K-FoxO-survivin axis and are sensitive to PI3K inhibitors. Cancer Res. 2013; 73:1190–200. [PubMed: 23204226]
18. Korkaya H, Paulson A, Iovino F, Wicha MS. HER2 regulates the mammary stem/progenitor cell population driving tumorigenesis and invasion. Oncogene. 2008; 27:6120–30. [PubMed: 18591932]
19. Paik S, Kim C, Wolmark N. HER2 status and benefit from adjuvant trastuzumab in breast cancer. N Engl J Med. 2008; 358:1409–11. [PubMed: 18367751]
20. Perez EA, Reinholz MM, Hillman DW, Tenner KS, Schroeder MJ, Davidson NE, et al. HER2 and chromosome 17 effect on patient outcome in the N9831 adjuvant trastuzumab trial. J Clin Oncol. 2010; 28:4307–15. [PubMed: 20697084]
21. Lukacs RU, Goldstein AS, Lawson DA, Cheng D, Witte ON. Isolation, cultivation and characterization of adult murine prostate stem cells. Nat Protoc. 2010; 5:702–13. [PubMed: 20360765]
22. Webster JA, Beck AH, Sharma M, Espinosa I, Weigelt B, Schreuder M, et al. Variations in stromal signatures in breast and colorectal cancer metastases. The Journal of pathology. 2010; 222:158–65. [PubMed: 20593409]
23. Holmes S, Kapelner A, Lee PP. An Interactive Java Statistical Image Segmentation System: GemIdent. Journal of statistical software. 2009:30.
24. Vaillant F, Asselin-Labat ML, Shackleton M, Forrest NC, Lindeman GJ, Visvader JE. The mammary progenitor marker CD61/beta3 integrin identifies cancer stem cells in mouse models of mammary tumorigenesis. Cancer Res. 2008; 68:7711–7. [PubMed: 18829523]
25. Clarke MF, Dick JE, Dirks PB, Eaves CJ, Jamieson CH, Jones DL, et al. Cancer stem cells--perspectives on current status and future directions: AACR Workshop on cancer stem cells. Cancer Res. 2006; 66:9339–44. [PubMed: 16990346]
26. Sauter G, Lee J, Bartlett JM, Slamon DJ, Press MF. Guidelines for human epidermal growth factor receptor 2 testing: biologic and methodologic considerations. J Clin Oncol. 2009; 27:1323–33. [PubMed: 19204209]
27. Shackleton M, Vaillant F, Simpson KJ, Stingl J, Smyth GK, Asselin-Labat ML, et al. Generation of a functional mammary gland from a single stem cell. Nature. 2006; 439:84–8. [PubMed: 16397499]
28. Stingl J, Eirew P, Ricketson I, Shackleton M, Vaillant F, Choi D, et al. Purification and unique properties of mammary epithelial stem cells. Nature. 2006; 439:993–7. [PubMed: 16395311]
29. Engreitz JM, Chen R, Morgan AA, Dudley JT, Mallelwar R, Butte AJ. ProfileChaser: searching microarray repositories based on genome-wide patterns of differential expression. Bioinformatics. 2011; 27:3317–8. [PubMed: 21967760]
30. Jani JP, Finn RS, Campbell M, Coleman KG, Connell RD, Currier N, et al. Discovery and pharmacologic characterization of CP-724,714, a selective ErbB2 tyrosine kinase inhibitor. Cancer Res. 2007; 67:9887–93. [PubMed: 17942920]
31. Levitzki A, Gazit A. Tyrosine kinase inhibition: an approach to drug development. Science. 1995; 267:1782–8. [PubMed: 7892601]
32. Wilson TR, Lee DY, Berry L, Shames DS, Settleman J. Neuregulin-1-mediated autocrine signaling underlies sensitivity to HER2 kinase inhibitors in a subset of human cancers. Cancer Cell. 2011; 20:158–72. [PubMed: 21840482]
33. Barretina J, Caponigro G, Stransky N, Venkatesan K, Margolin AA, Kim S, et al. The Cancer Cell Line Encyclopedia enables predictive modelling of anticancer drug sensitivity. Nature. 2012; 483:603–7. [PubMed: 22460905]

34. Prat A, Parker JS, Karginova O, Fan C, Livasy C, Herschkowitz JI, et al. Phenotypic and molecular characterization of the claudin-low intrinsic subtype of breast cancer. Breast Cancer Res. 2010; 12:R68. [PubMed: 20813035]
35. Atlas E, Cardillo M, Mehmi I, Zahedkargaran H, Tang C, Lupu R. Heregulin is sufficient for the promotion of tumorigenicity and metastasis of breast cancer cells in vivo. Mol Cancer Res. 2003; 1:165–75. [PubMed: 12556556]
36. Tsai MS, Shamon-Taylor LA, Mehmi I, Tang CK, Lupu R. Blockage of heregulin expression inhibits tumorigenicity and metastasis of breast cancer. Oncogene. 2003; 22:761–8. [PubMed: 12569369]
37. Hinohara K, Kobayashi S, Kanauchi H, Shimizu S, Nishioka K, Tsuji E, et al. ErbB receptor tyrosine kinase/NF-kappaB signaling controls mammosphere formation in human breast cancer. Proc Natl Acad Sci U S A. 2012; 109:6584–9. [PubMed: 22492965]
38. Nakanishi T, Chumsri S, Khakpour N, Brodie AH, Leyland-Jones B, Hamburger AW, et al. Side-population cells in luminal-type breast cancer have tumour-initiating cell properties, and are regulated by HER2 expression and signalling. Br J Cancer. 2010; 102:815–26. [PubMed: 20145614]
39. Ithimakin S, Day KC, Malik F, Zen Q, Dawsey SJ, Bersano-Begey TF, et al. HER2 Drives Luminal Breast Cancer Stem Cells in the Absence of HER2 Amplification: Implications for Efficacy of Adjuvant Trastuzumab. Cancer Res. 2013; 73:1635–46. [PubMed: 23442322]
40. Dalerba P, Dylla SJ, Park IK, Liu R, Wang X, Cho RW, et al. Phenotypic characterization of human colorectal cancer stem cells. Proc Natl Acad Sci U S A. 2007; 104:10158–63. [PubMed: 17548814]
41. de Alava E, Ocana A, Abad M, Montero JC, Esparis-Ogando A, Rodriguez CA, et al. Neuregulin expression modulates clinical response to trastuzumab in patients with metastatic breast cancer. J Clin Oncol. 2007; 25:2656–63. [PubMed: 17602072]
42. Menendez JA, Mehmi I, Lupu R. Trastuzumab in combination with heregulin-activated Her-2 (erbB-2) triggers a receptor-enhanced chemosensitivity effect in the absence of Her-2 overexpression. J Clin Oncol. 2006; 24:3735–46. [PubMed: 16847284]
43. Wulfkuhle JD, Berg D, Wolff C, Langer R, Tran K, Illi J, et al. Molecular analysis of HER2 signaling in human breast cancer by functional protein pathway activation mapping. Clin Cancer Res. 2012; 18:6426–35. [PubMed: 23045247]

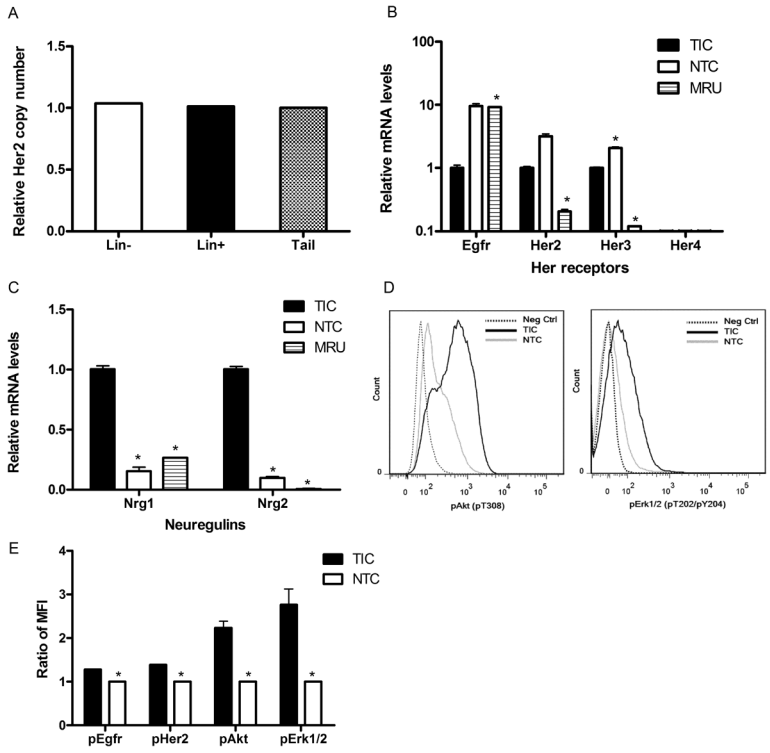

Figure 1. Neuregulins are overexpressed in CD24^{Hi}CD49f^{Hi} TIC-enriched cells

(A) Bar graph showing Her2 status in MMTV-*Wnt1* mice. *Her2* gene copy number was determined by quantitative PCR analysis using 10ng genomic DNA extracted from lineage-negative (Lin−) cancer cells and lineage-positive (Lin+) stromal cells or a tail sample. (B) Expression levels of Egfr, Her2, Her3 and Her4 in mammary repopulating unit (MRU)-enriched cells from mouse normal mammary glands and CD24^{Hi}CD49f^{Hi} TIC-enriched cells and NTCs isolated from MMTV-*Wnt1* tumors ($p<0.03$). (C) Neuregulin mRNA expression levels in MRU-enriched, CD24^{Hi}CD49f^{Hi} TIC-enriched and NTC populations ($p<0.04$). RT-PCR was performed in duplicates on five biological tumor replicates from independent mice. (D) FACS histogram plots showing the levels of pAkt and pErk1/2 in TICs and NTCs. (E) Bar graph showing the ratios of median fluorescent intensity (MFI) of pEgfr, pHer2, pAkt and pErk1/2 normalized to Egfr, Her2, Akt, and Erk1/2, respectively ($p<0.001$). Results are shown as mean ± SEM.

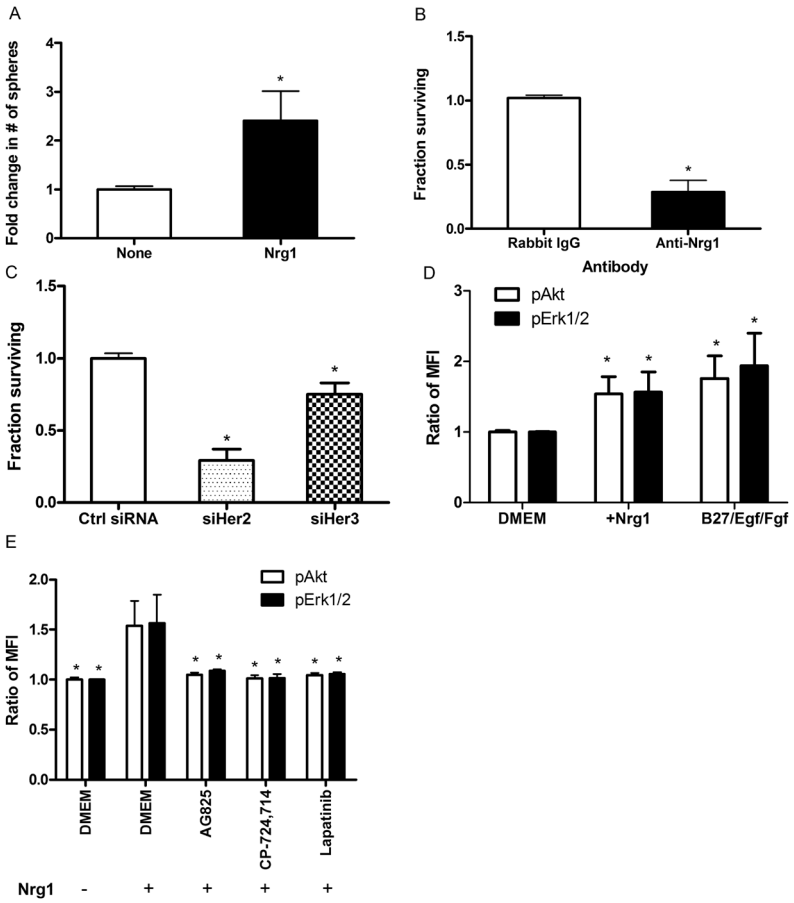

Figure 2. Nrg1 stimulates the self-renewal and proliferation of $CD24^{Hi}CD49f^{Hi}$ TIC-enriched cells through Her3 and activation of Akt and Erk1/2 pathways

(A) *In vitro* sphere forming assay showing Nrg1 (100ng/mL) stimulated $CD24^{Hi}CD49f^{Hi}$ TIC-enriched cell proliferation (n = 6, $p<0.05$). (B) Sphere forming assay showing the inhibitory effect of anti-Nrg1 antibody. $CD24^{Hi}CD49f^{Hi}$ TIC-enriched cells were cultured in the presence of 4μg/mL normal rabbit IgG or anti-Nrg1 antibodies (n = 7, $p<0.001$). (C) Sphere forming assay showing the effect of Her2 and Her3 knockdown. $CD24^{Hi}CD49f^{Hi}$ TIC-enriched cells were treated with 1μM siRNA (n = 5, $p<0.04$). (D) $CD24^{Hi}CD49f^{Hi}$ TIC-enriched cells were cultured in standard medium (B27/Egf/Fgf) or Nrg1 (100ng/mL) in low cluster plate for 30 min. at 37°C. pAkt and pErk1/2 levels were determined by phospho-flow analysis (n = 4, $p<0.05$). (E) Bar graph showing the effect of Nrg1 on the phosphorylation and activation of Akt and Erk1/2 pathways. $CD24^{Hi}CD49f^{Hi}$ TIC-enriched cells were starved for 30 min. and then stimulated with Nrg1 (100ng/mL) for 30min. at 37°C. pAkt and pErk1/2 levels were then determined by phospho-flow analysis. For drug treatments, $CD24^{Hi}CD49f^{Hi}$ TIC-enriched cells were pretreated with AG825 (100μM), CP-724,714 (5μM) and Lapatinib (5μM) for 10min at 37°C in DMEM and then stimulated with Nrg1 (100ng/mL). Bars represent mean ± SEM (n = 5, $p<0.05$).

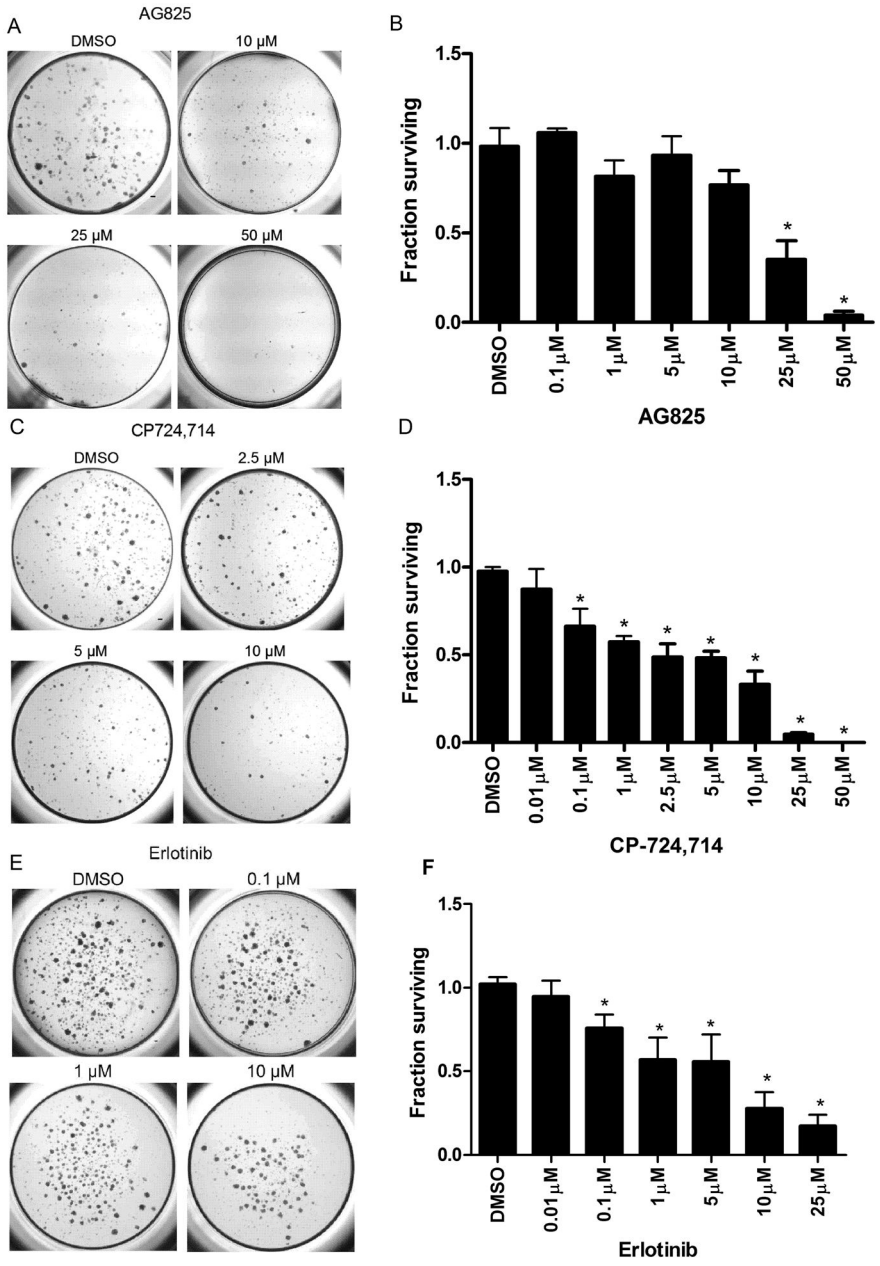

Figure 3. Targeting Her2 inhibits the proliferation of $CD24^{Hi}CD49f^{Hi}$ TIC-enriched cells

(A) Representative images of $CD24^{Hi}CD49f^{Hi}$ TIC-enriched cells treated with AG825 at varying concentrations (0, 10, 25 and 50μM) in *in-vitro* sphere forming assays. Bar denotes 100μm. (B) Bar graph showing that AG825 reduced the spheroid forming abilities of $CD24^{Hi}CD49f^{Hi}$ TIC-enriched cells at a concentration of 25μM (n = 4, $p<0.001$). Bars represent mean ± SEM. (C) Representative images of $CD24^{Hi}CD49f^{Hi}$ TIC-enriched cells treated with CP-724,714 at varying concentrations (0, 2.5, 5 and 10μM) in *in-vitro* sphere forming assays. Bar denotes 100μm. (D) Bar graph showing that CP-724,714 reduced the sphere forming abilities of $CD24^{Hi}CD49f^{Hi}$ TIC-enriched cells at a concentration of 10μM (n = 3, $p<0.01$). (E) Representative images of $CD24^{Hi}CD49f^{Hi}$ TIC-enriched cells treated with erlotinib at varying concentrations (0, 0.1, 1 and 10μM) in *in-vitro* sphere forming

assays. Bar denotes 100μm. (F) Bar graph showing that erlotinib reduced the sphere forming abilities of $CD24^{Hi}CD49f^{Hi}$ TIC-enriched cells at a concentration of 10μM (n = 3, $p<0.02$).

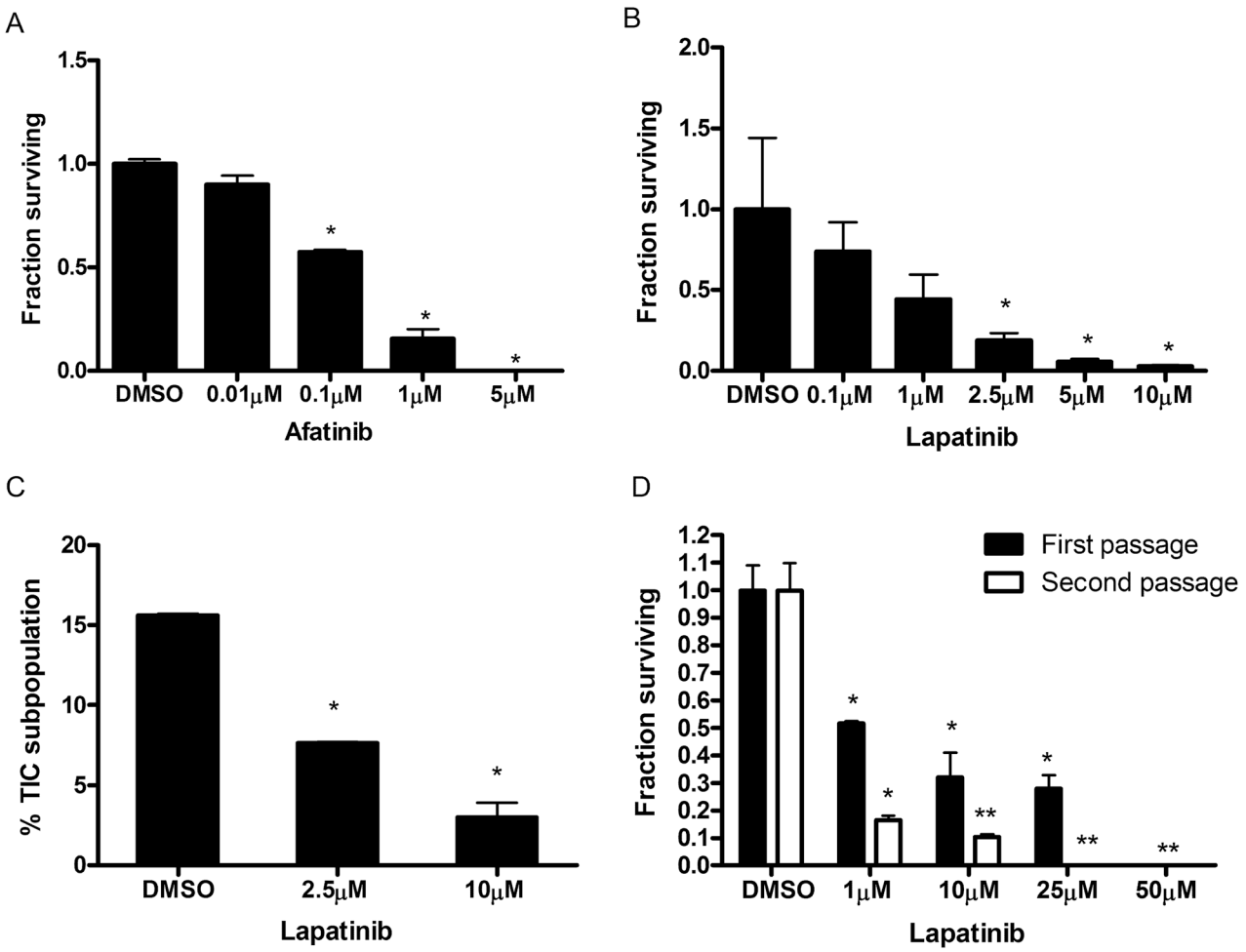

Figure 4. Lapatinib inhibited the capability of $CD24^{Hi}CD49f^{Hi}$ TIC-enriched cells to proliferate and self-renew

(A) Bar graph showing that afatinib reduced the sphere forming abilities of $CD24^{Hi}CD49f^{Hi}$ TIC-enriched cells at a concentration of 1μM (n = 3, $p<0.02$). Bars represent mean ± SEM. (B) *In vitro* sphere forming assay showing the dose-dependent effect of lapatinib in $CD24^{Hi}CD49f^{Hi}$ TIC-enriched cells. Cells were treated with lapatinib at varying doses (0, 0.1, 1, 2.5, 5 and 10μM) in the *in vitro* sphere forming assay (n = 3, $p<0.03$). (C) Bar graph showing the percentage of $CD24^{Hi}CD49f^{Hi}$ TIC-enriched cells in tumors treated with lapatinib at 2.5μM and 10μM (n = 3, $p<0.002$). (D) *In vitro* self-renewal assay showing the inhibitory effect of lapatinib on self-renewal of $CD24^{Hi}CD49f^{Hi}$ TIC-enriched cells. Cells were treated with lapatinib at 0, 0.1, 1, 2.5, 5 and 10 μM and the fraction of surviving spheres was determined (n = 3, *$p<0.02$). Spherical colonies from the first passage were then dissociated into single cells and re-plated in the second passage without lapatinib treatment (n = 3, * $p<0.04$, **$p< 0.001$). Bars represent mean ± SEM.

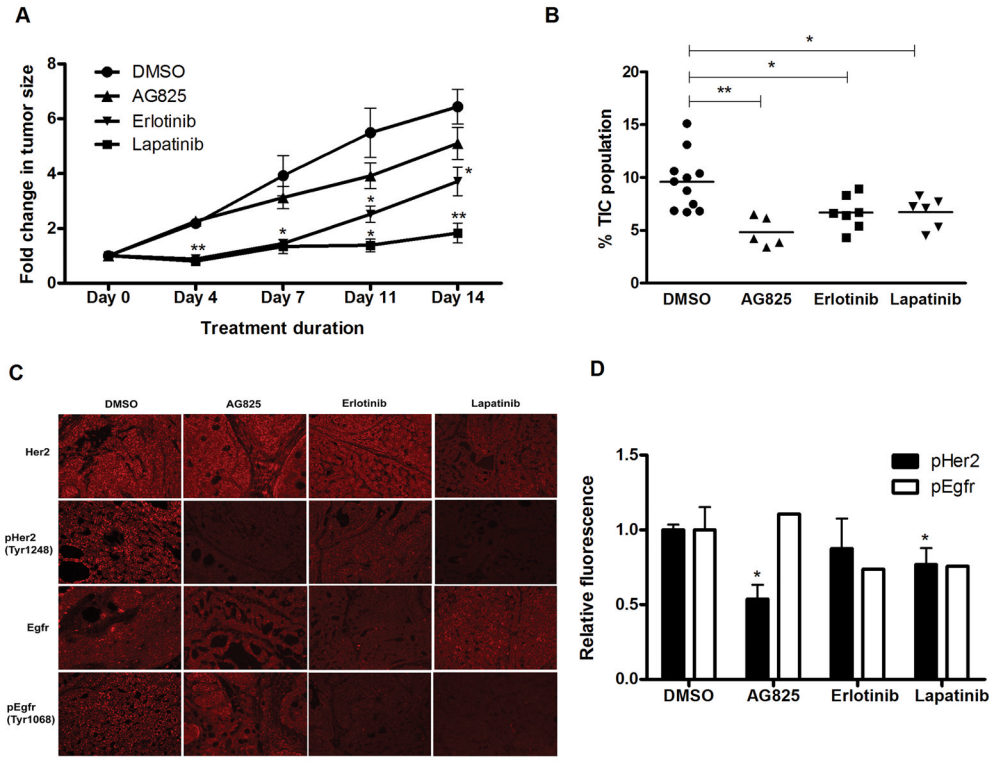

Figure 5. Dual inhibition of Her2 and Egfr suppresses tumor growth and reduces the percentage of $CD24^{Hi}CD49f^{Hi}$ TIC-enriched cells *in vivo*

(A) Tumor growth assay showing the effect of AG825, erlotinib and lapatinib. Mice bearing MMTV-*Wnt1* tumors were treated with DMSO (n = 5), AG825 (50μg/kg, n = 5) once daily via intraperitoneal administration, erlotinib (100mg/kg, n = 7) once daily via oral gavage or lapatinib (100mg/kg, n = 6) twice daily via oral gavages. Tumor size was determined by caliper measurements twice weekly (* $p<0.01$, ** $p<0.001$). (B) Scatter plots showing the percentage of $CD24^{Hi}CD49f^{Hi}$ TIC-enriched cells in tumors treated with DMSO, AG825, erlotinib or lapatinib. Tumors were dissociated into single cells at the end of treatment period and analyzed by FACS analysis (* $p<0.01$; ** $p<0.001$). (C) Immunohistochemical images at 200x magnification showing expression levels of Egfr, pEgfr, Her2 and pHer2 of tumors sections (5μm) harvested at the end (day 14) of DMSO, AG825, erlotinib or lapatinib treatment. (D) Bar graph showing the relative fluorescence of pHer2 and pEgfr in tumors treated with DMSO, AG825, erlotinib or lapatinib ($p<0.05$). Bars represent mean ± SEM.

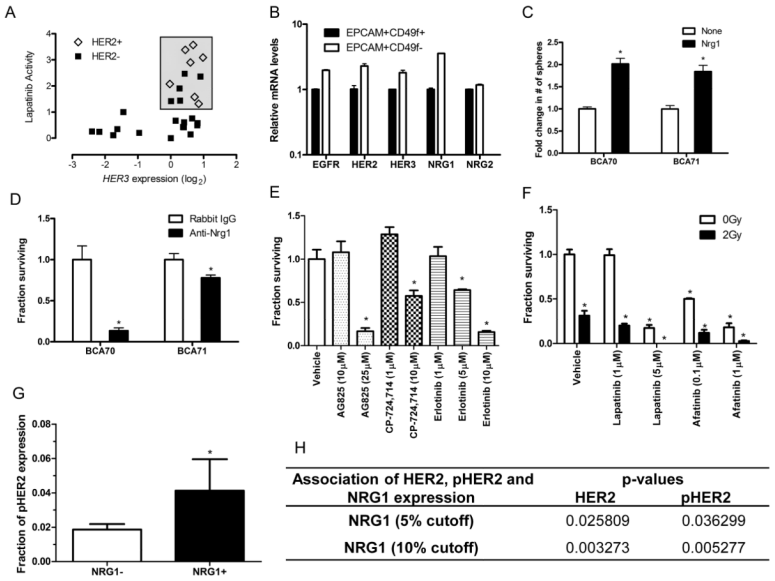

H

Association of HER2, pHER2 and NRG1 expression	p-values	
	HER2	pHER2
NRG1 (5% cutoff)	0.025809	0.036299
NRG1 (10% cutoff)	0.003273	0.005277

Figure 6. HER2 inhibition targets a subset of human HER2-low breast cancer cell lines and breast TICs in patient-derived xenografts

(A) Relative expression of *HER3* and activity of lapatinib in 7 *HER2*-amplified and 20 *HER2*-non-amplified breast cancer cell lines from the Cancer Cell Line Encyclopedia. The box highlights lapatinib-sensitive cell lines. (B) Expression levels of HER receptors and neuregulins in patient-derived xenograft breast tumors (n = 3). (C) *In vitro* sphere forming assay showing NRG1 (100ng/mL) stimulated patient-derived xenografts BCA70 (n = 3, $p<0.01$) and BCA71 (n = 4, $p<0.001$) TIC-enriched cell proliferation (D) Sphere forming assay showing the inhibitory effect of anti-NRG1 antibody. TIC-enriched cells from BCA70 (n = 6, $p<0.01$) and BCA71 (n = 4, $p<0.02$) were cultured in the presence of 4μg/mL normal rabbit IgG or anti-NRG1 antibodies. (E) Bar graph showing that AG825 (25μM), CP-724,714 (10μM) and Erlotinib (5μM, 10 μM) reduced the sphere forming abilities of BCA70 TIC-enriched cells (n = 3, $p<0.02$). Bars represent mean ± SEM. (F) Clonogenic survival assays of BCA70 TIC-enriched cells in the presence of ionizing radiation (2Gy) with or without lapatinib or afatinib treatment (* $p<0.001$). Bars represent mean ± SEM. (G) Tissue microrarray analysis of 132 HER2-low breast cancers. Bar graph showing fraction of pHER2 expression in HER2-low breast tumors stratified by NRG1 expression with a cutoff of 5% expression level ($p<0.04$). (H) Association between NRG1, HER2 and pHER2 expression levels in HER2-negataive tumors stratified by NRG1 expression.

Table 1

In vivo limiting dilution analysis of lineage-negative mammary tumor cells after treatment with DMSO, AG825, erlotinib or lapatinib (* $p<0.01$).

Treatment Groups	# cells injected	# tumor formation/total # injections	TIC frequency
DMSO	100	0/5	**1/633** (1/404–1/991)
	500	3/5	
	2,500	5/5	
	5,000	5/5	
AG825	100	0/5	**1/2,641*** (1/1,813 – 1/3,847)
	500	1/5	
	2,500	2/5	
	5,000	5/5	
Erlotinib	100	0/5	**1/2,715*** (1/1,739 – 1/4,239)
	500	0/5	
	1,000	2/5	
	2,000	3/5	
Lapatinib	100	0/5	**1/3,837*** (1/2,307 – 1/6,381)
	500	0/5	
	1,000	3/5	
	2,000	1/5	